

A detailed study of charm content of a proton in the frameworks of the *Kimber-Martin-Ryskin* and *Martin-Ryskin-Watt* approaches

N. Olanj^{†*} and M. Modarres[‡]

[†]*Physics Department, Faculty of Science,*

Bu-Ali Sina University, 65178, Hamedan, Iran and

[‡]*Physics Department, University of Tehran, 1439955961, Tehran, Iran.*

Abstract

The charm structure function, $(F_2^{c\bar{c}}(x, Q^2))$, is calculated in the framework of the k_t -factorization formalism by using the *unintegrated* parton distribution functions (*UPDF*), which are generated through the *Kimber et al. (KMR)* and *Martin et al. (MRW)* procedures. The *Martin* group (*MMHT2014*) parton distribution functions (*PDF*) is used as the input *PDF* for the corresponding *UPDF*. The resulted $F_2^{c\bar{c}}(x, Q^2)$ is compared with the predicted data and the calculations given by the *ZEUS* and *H1* collaborations, the parton *pQCD* theory, i.e. the general-mass variable-flavour-number scheme (*GMVFNS*), the *LO* collinear procedure and the saturation model introduced by *Golec – Biernat* and *Wüsthoff (GBW)*, respectively. In general, it is shown that the calculated charm structure functions based on the stated above two *UPDF* schemes are consistent with the experimental data and other theoretical predictions. Also, a short discussion is presented regarding the *KMR* and *MRW UPDF* behaviors.

PACS numbers: 12.38.Bx, 13.85.Qk, 13.60.-r

Keywords: k_t -factorization, *unintegrated* parton distribution, *DGLAP* equation, charm structure function

*Corresponding author, Email : n_olanj@basu.ac.ir , Tel:+98-81-38381601

I. INTRODUCTION

The heavy-quark electro-production contributes up to 25 % to the deep inelastic scattering (*DIS*) inclusive cross section at small x [1]. Therefore, the study of the heavy-quark distribution functions of hadrons become a significant gradient in the *Higgs* production [2] at the *LHC* and in the *W* and *Z* bosons inclusive production [3, 4]. So the measurement of the heavy quarks structure functions in *DIS* at *HERA* is an important test of the theory of perturbative quantum *chromodynamics* (*pQCD*) at the small *Bjorken* scale [4, 5] as well as the outcome of the above *LHC* semi-inclusive cross sections.

Usually, *pQCD* is applied to calculate various quantities such the hadrons structure function, the hadron-hadron differential cross sections, etc., but, as we pointed out above, it is well known that in the small *Bjorken* scale region, there are some theoretical problems [6–8], which indicate that transverse momentum and the reggeon play an important role [6–8]. In recent years, plenty of available experimental data on the various events, such as the exclusive and semi-inclusive processes in the high energy collisions at *LHC*, indicates the necessity for computation of the transverse-dependent parton distributions, which are called the *unintegrated* parton distribution functions (*UPDF*). Therefore, the extraction of the *UPDF* recently become very important. The *UPDF*, $f_a(x, k_t^2, \mu^2)$, are the two-scale dependent functions, i.e., k_t^2 and μ^2 , which satisfy the *Ciafaloni-Catani-Fiorani-Marchesini* (*CCFM*) equations [9–12], where x , k_t , and μ are the longitudinal momentum fraction (the *Bjorken* variable), the transverse momentum, and the factorization scale, respectively. Nevertheless, solving the *CCFM* equation is a mathematically involved task. Also, there is not a complete quark version of the *CCFM* formalism. Therefore, to obtain the *UPDF*, the *Kimber, Martin and Ryskin* (*KMR*) [13] and the *Martin, Ryskin and Watt* (*MRW*) [14] proposed a different procedure based on the standard *Dokshitzer-Gribov-Lipatov-Altarelli-Parisi* (*DGLAP*) equations [15–18] in the leading order (*LO*) and the next-to-leading order (*NLO*) levels, respectively, along with a modification due to the angular ordering condition (*AOC*), which is the key dynamical property of the *CCFM* formalism. As evidenced by the analytic extraction of the parton distribution functions from the evolution equation (the *DGLAP* equation) in the reference [4], the integration over the transverse momentum of the partons are performed. Therefore, the *UPDF*, f_a unintegrated over the parton k_t , are the fundamental quantities for the phenomenological computations in the

high energy collisions of hadrons.

Due to the importance of this subject, in the present work, by studying recent data on charm structure functions at the small x , we examine the validity of the KMR and MRW approaches.

In our previous articles, we investigated the general behavior and stability of the KMR and MRW schemes [19–27]. Also, we have successfully used $KMR-UPDF$ to calculate the inclusive production of the W and Z gauge vector bosons [28, 29], the semi- NLO production of $Higgs$ bosons [30], the production of forward-center and forward-forward di-jets [31], the prompt-photon pair production [32] and recently in the reference [33], we explored the phenomenology of the integral and the differential versions of the $KMR-UPDF$ using the angular (strong) ordering (AOC (SOC)) constraints. But here, to check the reliability of generated $UPDF$, we use them to calculate the observable, deep inelastic scattering the charm structure functions ($F_2^{c\bar{c}}(x, Q^2)$). Then the predictions of these two methods for the charm structure functions are compared to the experimental measurements of $ZEUS$ [5] and $H1$ [34] as well as the parton model $pQCD$, i.e., the general-mass variable-flavour-number scheme ($GMVFNS$) [35–40] and the saturation model introduced by *Golec – Biernat* and *Wüsthoff* (GBW) [41].

The $UPDF$ are prepared using the $MMHT2014$ [42] set of parton distribution function (PDF) in the LO and NLO levels.

So, the paper is organized as follows: in the section *II*, a glimpse of the KMR and MRW approaches for the calculation of the double-scale $UPDF$ is presented. The formulation of $F_2^{c\bar{c}}(x, Q^2)$ based on the k_t -factorization ([43–47]) scheme is given in the section *III*. Finally, the results, as well as our discussions and conclusions, are given in the section *IV*.

II. A GLIMPSE OF THE KMR AND MRW APPROACHES

The KMR [13] and MRW [14] formalisms were developed to generate the $UPDF$, $f_a(x, k_t^2, \mu^2)$, by using the given PDF , ($a(x, \mu^2) = xq(x, \mu^2)$ and $xg(x, \mu^2)$), and the corresponding splitting functions $P_{aa'}(x)$ at the LO and NLO levels, respectively, such that the equation (1) [13, 48] is satisfied:

$$a(x, Q^2) = \int_0^{Q^2} \frac{dk_t^2}{k_t^2} f_a(x, k_t^2, Q^2), \quad (1)$$

since the $UPDF$ can only be defined in the perturbative regime $k_t > Q_0$, the integral in the equation (1) will be from Q_0^2 to Q^2 , and therefore the left-hand side of this equation is converted to $a(x, Q^2) - a(x, Q_0^2)$.

It should be noted that the k_t -integrals of the $UPDF$ (the f_q and f_g functions) obtained by the KMR and the MRW approaches are only approximately equal to the integrated ordinary PDF (q and g) that come from a global fit to data using the conventional collinear approximation. As it is stated in the reference [14], the two sides of the equation (1) are mathematically equivalent as far as we neglect the singularity of the splitting functions, $P_{qq}(z)$ and $P_{gg}(z)$, at $z = 1$, corresponding to the soft gluon emission. Otherwise, by considering the singularity of the splitting functions and consequently the cutoff, according to the reference [49], the difference between the two sides of the equation (1) can be eliminated by using the cutoff dependent PDF , that comes from a global fit to data using the k_t -factorization procedures, instead of the ordinary PDF . We show in the table 1, that the discrepancy between the k_t -integrals of the KMR - $UPDF$ (for the gluon and the up and charm quarks) with the input $MMHT2014 - LO$ PDF and their corresponding $MMHT2014 - LO$ PDF lies approximately in the uncertainty band of $MMHT2014 - LO$ PDF [42]. According to the reference [50], the use of ordinary integrated PDF is adequate for the initial investigations and descriptions of exclusive processes. Also, we have shown in the reference [33] that the usual global fitted PDF instead of the cutoff dependent PDF can be used for generating the $UPDF$ of the integral version of the KMR approach with the AOC constraint with good approximation.

These two procedures, which are reviewed in this section, are the modifications to the standard $DGLAP$ evolution equations by imposing the AOC , which is the consequence of the coherent gluon emissions.

Therefore, in the KMR approach, the separation of the real and virtual contributions in the $DGLAP$ evolution chain at the LO level, leads to the following forms for the quark and gluon $UPDF$:

$$\begin{aligned}
f_q(x, k_t^2, \mu^2) &= T_q(k_t, \mu) \frac{\alpha_s(k_t^2)}{2\pi} \\
&\times \int_x^{1-\Delta} dz \left[P_{qq}(z) \frac{x}{z} q\left(\frac{x}{z}, k_t^2\right) \right. \\
&\left. + P_{qg}(z) \frac{x}{z} g\left(\frac{x}{z}, k_t^2\right) \right], \tag{2}
\end{aligned}$$

$$\begin{aligned}
f_g(x, k_t^2, \mu^2) &= T_g(k_t, \mu) \frac{\alpha_s(k_t^2)}{2\pi} \\
&\times \int_x^{1-\Delta} dz \left[\sum_q P_{gq}(z) \frac{x}{z} q\left(\frac{x}{z}, k_t^2\right) \right. \\
&\left. + P_{gg}(z) \frac{x}{z} g\left(\frac{x}{z}, k_t^2\right) \right], \tag{3}
\end{aligned}$$

respectively, where $P_{aa'}(x)$ are the corresponding splitting functions, and the survival probability factors, T_a , are evaluated from:

$$\begin{aligned}
T_a(k_t, \mu) &= \exp \left[- \int_{k_t^2}^{\mu^2} \frac{\alpha_s(k_t'^2)}{2\pi} \frac{dk_t'^2}{k_t'^2} \right. \\
&\left. \times \sum_{a'} \int_0^{1-\Delta} dz' P_{a'a}(z') \right]. \tag{4}
\end{aligned}$$

The *AOC* on the last step of the evolutionary process determined the cutoff, $\Delta = 1 - z_{max} = \frac{k_t}{\mu + k_t}$, to prevent $z = 1$ singularities in the splitting functions [13], which arises from the soft gluon emission. In the *KMR* approach, T_a is considered to be unity for $k_t > \mu$. This constraint and its interpretation in terms of the strong ordering condition gives the *KMR* approach a smooth behavior over the small- x region, which is generally governed by the *Balitski – Fadin – Kuraev – Lipatov (BFKL)* evolution equation [51, 52].

In the *MRW* approach [14], the same separation of real and virtual contributions to the *DGLAP* evolution is done, but the procedure is at the *NLO* level, i.e.,

$$\begin{aligned}
f_a(x, k_t^2, \mu^2) &= \int_x^1 dz T_a(k^2, \mu^2) \frac{\alpha_s(k^2)}{2\pi} \\
&\times \sum_{b=q,g} P_{ab}^{(0+1)}(z) b\left(\frac{x}{z}, k^2\right) \Theta(\mu^2 - k^2), \tag{5}
\end{aligned}$$

where

$$\begin{aligned}
P_{ab}^{(0+1)}(z) &= P_{ab}^{(0)}(z) + \frac{\alpha_s}{2\pi} P_{ab}^{(1)}(z), \\
k^2 &= \frac{k_t^2}{1-z}, \tag{6}
\end{aligned}$$

and

$$\begin{aligned}
T_a(k^2, \mu^2) &= \exp \left(- \int_{k^2}^{\mu^2} \frac{\alpha_s(\kappa^2)}{2\pi} \frac{d\kappa^2}{\kappa^2} \right. \\
&\left. \times \sum_{b=q,g} \int_0^1 d\zeta \zeta P_{ba}^{(0+1)}(\zeta) \right). \tag{7}
\end{aligned}$$

$P_{ab}^{(0)}$ and $P_{ab}^{(1)}$ functions in the above equations correspond to the *LO* and *NLO* contributions of the splitting functions, which are given in the reference [53], respectively.

It is evident from the equation (5) that, in the *MRW* approach, the *UPDF* are defined such that, to ensure $k^2 < \mu^2$. Therefore, the *MRW* approach is more in compliance with the *DGLAP* evolution equations requisites, unlike the *KMR* approach that the *AOC* spreads the *UPDF* to whole transverse momentum region, and it makes the results sum up the leading *DGLAP* and *BFKL* logarithms. Unlike the *KMR* approach, where the *AOC* is imposed on the all of the terms of the equations (2) and (3), in the *MRW* approach, the *AOC* is imposed by the terms in which the splitting functions are singular, i.e., the terms which include P_{qq} and P_{gg} .

III. THE FORMULATION OF $F_2^{c\bar{c}}(x, Q^2)$ IN THE k_t -FACTORIZATION APPROACH

Here we briefly describe the different steps for calculations of the charm structure functions, $F_2^{c\bar{c}}(x, Q^2)$, in the k_t -factorization approach [54]. Since the gluons in the proton can only contribute to $F_2^{c\bar{c}}(x, Q^2)$ through the intermediate quark, so one should calculate the charm structure functions in the k_t -factorization approach by using the gluons and quarks *UPDF*. In this level, there are six diagrams corresponding to the subprocess $g \rightarrow q\bar{q}$ and $q \rightarrow qg$, (see the figure 6 of the reference [55]). Following these six diagrams [55], by considering a physical gauge for the gluon, i.e., $A^\mu q'_\mu = 0$ ($q' = q + xp$), only the ladder-type diagrams (for example the quark box and the crossed box approximations to the photon-gluon subprocess) remain valid for the calculation (see the figure 7 of the reference [22]). These contributions may be written in the k_t -factorization form, by using the *UPDF* which are generated through the *KMR* and *MRW* formalisms, as follows:

(i) For the gluons,

$$F_{2g \rightarrow q\bar{q}}^{c\bar{c}}(x, Q^2) = e_c^2 \frac{Q^2}{4\pi} \int \frac{dk_t^2}{k_t^4} \int_0^1 d\beta \int d^2\kappa_t \alpha_s(\mu^2) f_g\left(\frac{x}{z}, k_t^2, \mu^2\right) \Theta\left(1 - \frac{x}{z}\right) \left\{ [\beta^2 + (1 - \beta^2)] \left(\frac{\kappa_t}{D_1} - \frac{(\kappa_t - \mathbf{k}_t)}{D_2} \right)^2 + [m_c^2 + 4Q^2\beta^2(1 - \beta)^2] \left(\frac{1}{D_1} - \frac{1}{D_2} \right)^2 \right\}, \quad (8)$$

where, in the above equation, in which the graphical representations of k_t and κ_t are introduced in the figure 7 of the reference [22], the variable β is defined as the light-cone fraction

of the photon momentum carried by the internal quark [13]. Also, the denominator factors are

$$\begin{aligned} D_1 &= \kappa_t^2 + \beta(1 - \beta)Q^2 + m_c^2, \\ D_2 &= (\kappa_t - \mathbf{k}_t)^2 + \beta(1 - \beta)Q^2 + m_c^2, \end{aligned} \quad (9)$$

and

$$\frac{1}{z} = 1 + \frac{\kappa_t^2 + m_c^2}{(1 - \beta)Q^2} + \frac{k_t^2 + \kappa_t^2 - 2\kappa_t \cdot \mathbf{k}_t + m_c^2}{\beta Q^2}. \quad (10)$$

As in the reference [56], the scale μ controls both the unintegrated partons and the QCD coupling constant (α_s), and in the former case, it is chosen as follows,

$$\mu^2 = k_t^2 + \kappa_t^2 + m_q^2. \quad (11)$$

The charm quark mass is taken to be $m_c = 1.27 GeV$.

(ii) For the quarks,

$$\begin{aligned} F_{2q \rightarrow qg}^{c\bar{c}}(x, Q^2) &= e_c^2 \int_{k_0^2}^{Q^2} \frac{d\kappa_t^2}{\kappa_t^2} \frac{\alpha_s(\kappa_t^2)}{2\pi} \int_{k_0^2}^{\kappa_t^2} \frac{dk_t^2}{k_t^2} \int_x^{\frac{Q}{(Q+k_t)}} dz \\ &\quad \left[f_c\left(\frac{x}{z}, k_t^2, Q^2\right) + f_{\bar{c}}\left(\frac{x}{z}, k_t^2, Q^2\right) \right] P_{qq}(z). \end{aligned} \quad (12)$$

It should be noted that the above relations for the subprocess $g \rightarrow q\bar{q}$ and $q \rightarrow qg$ are true only for the region of the $pQCD$. But since we are working in the small x region or the equivalently, the high energy, the contribution of the non-*perturbative* region can be neglected, and the dominant mechanism of the proton c -quark electroproduction is the photon-gluon fusion (i.e. the subprocess $g \rightarrow q\bar{q}$).

Finally, the structure function $F_2^{c\bar{c}}(x, Q^2)$ can be calculated by the sum of gluons, the equation (8), and quarks, the equation (12), contributions.

IV. RESULTS, DISCUSSIONS AND CONCLUSIONS

As we pointed out before, the present work aim is to study the charm content of a proton in the frameworks of the *KMR* and *MRW* approaches and validate these two formalisms. In this regard, the charm structure functions, i.e., the sum of $F_{2g \rightarrow q\bar{q}}^{c\bar{c}}$ and $F_{2q \rightarrow qg}^{c\bar{c}}$ of the equations (8) and (12) are calculated by using the *UPDF* of the *KMR* and *MRW*

approaches, i.e., the equations (2), (3) and (5), respectively. In the panels (a) to (g) of figure 1, the charm structure functions, $F_2^{c\bar{c}}(x, Q^2)$, are displayed, by using the *KMR* (*KMR, MMHT2014 – LO*, dash curves) and *MRW* (*MRW, MMHT2014 – NLO*, full curves) approaches, as a function of x for different values of $Q^2=6.5, 12, 25, 30, 80, 160$ and 600 GeV^2 with the input *MMHT2014* set of *PDF* (to generate the *UPDF*) at the *LO* and *NLO* approximations, respectively. These results are compared with the data given by the *ZEUS* collaboration [5] and the *NLO-QCD HERAPDF 1.5* [40] predictions based on the general-mass variable- flavour-number scheme (*GMVFNS*). As one should expect, the results of the *KMR, MMHT2014 – LO* and *MRW, MMHT2014 – NLO* approaches are very close to each other at the low hard scale (Q^2), but they become separated as the hard scale increases. On the other hand, they are very close to the experimental data, i.e., the *ZEUS* (2014) data [5] (the full circle points). As we stated above, the general mass variable flavour number scheme (*HERAPDF 1.5 GMVFNS*, dash-dotted curve) *pQCD* calculation is also plotted for comparison. As it was noted in the reference [50], we do not expect to get a better results than *pQCD*, although the k_t -factorization is more computationally simplistic. It is worth noting that the discrepancy between the data and the k_t -factorization prediction can be reduced by refitting the input integrated *PDF*. As it has been explained in the reference [50], this treatment is adequate for initial investigations and descriptions of exclusive processes. In the panel (d) of this figure, a comparison is also made with the saturation model introduced by *Golec – Biernat* and *Wüsthoff* [41] (*GBW*, the dotted curve) and the old *ZEUS* (2000) data [57] (the filled squares). Again our calculations are consistent with them.

The charm structure functions, $F_2^{c\bar{c}}(x, Q^2)$, as a function of the hard scale Q^2 are also calculated in the *KMR* (dash curves), and *MRW* (full curves) approaches as a function of Q^2 for various x values through the set of *MMHT2014 PDF* as the inputs. In the figure 2, the obtained results are compared with the data given by the *H1* collaboration [34] (full circles) and the *GMVFNS QCD* predictions [35–39] of *MSTW* at *NNLO* [3] (dash-dotted curves). Again as Q^2 and x increase, the *MRW* prescription gives closer results with respect to those of *KMR* and the differences become larger. On the other hand, one can conclude that in general, the k_t -factorization and *pQCD* calculations are very closed and they are in agreement with the data.

Also, we calculate the charm structure functions, $F_2^{c\bar{c}}(x, Q^2)$ by using the *LO* collinear

factorization with the inputs *MMHT2014-LO PDF* and plot the results in the figures 1 and 2. As expected, at higher energies (Q^2), the compatibility between the k_t and collinear factorization calculations with the same *PDF* becomes greater.

To make the comparison more apparent between the frameworks of *KMR* and *MRW*, the typical input of the gluon and charm quark *PDF* at scale $Q^2 = 25\text{GeV}^2$, by using the *MMHT2014-LO* (dash curves) and *MMHT2014-NLO* [42] (full curves), are plotted in the figure 3, and the *KMR-UPDF* (dash curves) and *MRW-UPDF* (full curves) are plotted versus k_t^2 at typical values of $x = 0.1, 0.01$ and 0.001 and the factorization scale $Q^2 = 100\text{GeV}^2$ in the figure 4.

As shown in the figure 4 for the large values of x (see the panel (d)), the values of the *KMR-UPDF* are larger than the *MRW-UPDF* due to increasing the scale $k^2 = \frac{k_t^2}{1-z}$ relative to the scale k_t^2 . This increase in scale, reduces α_s and *PDF* and consequently decreases the *MRW-UPDF* relative to the *KMR-UPDF*. But in the panel (a), since the charm quark *PDF* of the *MMHT2014-NLO* are larger than the charm quark *PDF* of the *MMHT2014-LO* (see the figure 3), the *MRW-UPDF* increase relative to the *KMR-UPDF* at the small k_t^2 . But for the small values of x and the small k_t^2 , the scales of the two approaches (k_t^2 and k^2) are almost equal, and the difference in the *KMR-UPDF* and *MRW-UPDF* is related to how the cutoff (due to *AOC*) is applied. As it is mentioned in section II, unlike the *KMR* approach, in the *MRW* approach, the effect of Δ on the terms which include non-singular splitting functions is negligible. Therefore, the *MRW-UPDF* becomes larger than the *KMR-UPDF* ones at the small x . This increase is more pronounced for the charm-*UPDF* than the gluon-*UPDF*. In the explanation of this increase, it can be argued that, as shown in the figure 3, since at the small x , gluons are much larger than charm quarks, this increase should happen. Therefore, terms containing quarks in the equations (2), (3) and (5) can be ignored in comparison to those containing gluons. As a result, it is natural that both sets of the gluon-*UPDF* become very similar, but due to the presence of non-singular terms, such as $P_{qg} \times g$ in quark-*UPDF*, the charm-*UPDF* of the *MRW* approach becomes larger than the charm-*UPDF* of the *KMR* approach. Here, it should be noted that, as it was shown in the references [24–27], the *KMR* formalism suppresses the discrepancies between the inputs *PDF*. Therefore, although gluons are larger in the *LO* approximation than in the *NLO* approximation (see the figure 3), the *MRW-UPDF* are still larger than the *KMR-UPDF* (at the small k_t^2) because of the difference in the

use of the cutoff Δ . For the small k_t^2 , due to the increase in k^2 over k_t^2 , the lower limit of integral increases in the Sudakov form factor the equations (4) and (7), so power of the exponential function becomes smaller, and as a result the Sudakov form factor in the *MRW* approach increase relative to the Sudakov form factor of the *KMR* approach. Therefore, the *MRW-UPDF* becomes larger than the *KMR-UPDF* at the small k_t^2 , except for the large x region due to the decrease in the α_s and the *PDF* in the large scale k^2 . For large k_t^2 , due to the presence of the cutoff $k^2 < \mu^2$ in the *MRW* approach, the *MRW-UPDF* are smaller than *KMR-UPDF*. Given the structure function equation (F_2), since it is proportional to the expression $\frac{\alpha_s(\mu^2)}{k_t^2}$, so it is clear that the contribution of small k_t^2 is dominant. Therefore, given that the *MRW-UPDF* are larger than the *KMR-UPDF* in the small k_t^2 , the charm structure functions which are extracted from the *MRW* approach is larger than those of *KMR*. As we expected, and it is clear from figures 1 and 2, the difference is more significant in the larger Q^2 . As the figures 1 and 2 illustrate and we expected, since charm quark is mostly produced at high energies and therefore at small x , the use of the *UPDF* in the *NLO* approximation (*MRW-UPDF*) can be in better agreement with the experimental data.

In conclusion, we can conclude that the obtained results for the charm structure functions with the predictions of the k_t -factorization formalism by using the *unintegrated* parton distribution functions (*UPDF*), which are generated through the *KMR* and *MRW* procedures are in agreement with the predictions of the *pQCD* and the experimental data . But the charm structure functions, which are extracted from the *MRW* approach, have a better agreement to the experimental data with respect to that of *KMR*. In explaining the cause of this phenomena, we can conclude that: This happens because the *unintegrated* parton distribution functions of the *MRW* approach (at the small x and small k_t^2 regions, i.e., the c -quark production domain) are slightly larger than the *unintegrated* parton distribution functions of the *KMR* formalism [14], which is due to the use the scale k^2 instead of the scale k_t^2 and not imposing *AOC* constraint on non-singular terms in the *MRW-UPDF*.

Acknowledgments

NO would like to acknowledge the University of *Bu – AliSina* and Dr. *M. Hajivaliei* for their support. *MM* would also like to acknowledge the Research Council of University

of Tehran for the grants provided for him.

- [1] A. V. Kotikov, A. V. Lipatov, and N. P. Zotov, *Eur. Phys. J. C* **27** (2003) 219.
- [2] F. Maltoni, Z. Sullivan, and S. Willenbrock, *Phys. Rev. D* **67** (2003) 093005.
- [3] A. D. Martin, W. J. Stirling, R. S. Thorne and G. Watt, *Eur. Phys. J. C* **63** (2009) 189.
- [4] G. Pancheri and Y. N. Srivastava, *Eur. Phys. J. C* **17** (2017) 150.
- [5] ZEUS collaboration, H. Abramowicz et al., *JHEP* **09** (2014) 127.
- [6] S. Catani and F. Hautmann, *Nucl. Phys. B* **427** (1994) 475.
- [7] A. Donnachie, H. G. Dosch, P. V. Landshoff and O. Nachtmann, *Pomeron physics and QCD*, Cambridge University Press, Cambridge (2002).
- [8] A. Donnachie and P.V. Landshoff, *Eur. Phys. J. C* **77** (2017) 524.
- [9] M. Ciafaloni, *Nucl. Phys. B* **296** (1988) 49 .
- [10] S. Catani, F. Fiorani, and G. Marchesini, *Phys. Lett. B* **234** (1990) 339.
- [11] S. Catani, F. Fiorani, and G. Marchesini, *Nucl. Phys. B* **336** (1990) 18.
- [12] G. Marchesini, *Nucl. Phys. B* **445** (1995) 49.
- [13] M. A. Kimber, A. D. Martin, and M. G. Ryskin, *Phys. Rev. D* **63** (2001) 114027.
- [14] A. D. Martin, M. G. Ryskin, and G.Watt, *Eur. Phys. J. C* **66** (2010) 163.
- [15] V.N. Gribov and L.N. Lipatov, *Yad. Fiz.*, **15** (1972) 781.
- [16] L.N. Lipatov, *Sov. J. Nucl. Phys.*, **20** (1975) 94.
- [17] G. Altarelli and G. Parisi, *Nucl. Phys. B*, **126** (1977) 298.
- [18] Y.L. Dokshitzer, *Sov.Phys.JETP*, **46** (1977) 641.
- [19] H. Hosseinkhani, M. Modarres, N. Olanj, *IJMPA* **32** (2017) 1750121.
- [20] M. Modarres, M. R. Masouminia, H. Hosseinkhani, N. Olanj, *Nucl. Phys. A* **945** (2016) 168.
- [21] M. Modarres, H. Hosseinkhani, N. Olanj, M.R. Masouminia, *Eur. Phys. J. C* **75** (2015) 556.
- [22] M. Modarres, H. Hosseinkhani, and N. Olanj, *Phys. Rev. D* **89** (2014) 034015.
- [23] M. Modarres, H. Hosseinkhani, and N. Olanj, *Nucl. Phys. A* **902** (2013) 21.
- [24] M. Modarres and H. Hosseinkhani, *Few-Body Syst.*, **47** (2010) 237.
- [25] M. Modarres and H. Hosseinkhani, *Nucl. Phys. A* **815** (2009) 40.
- [26] H. Hosseinkhani and M. Modarres, *Phys. Lett. B* **694** (2011) 355.
- [27] H. Hosseinkhani and M. Modarres, *Phys. Lett. B* **708** (2012) 75.

- [28] M. Modarres, M. R. Masouminia, R. Aminzadeh-Nik, H. Hoseinkhani, N. Olanj, Phys. Rev. D **94** (2016) 074035.
- [29] M. Modarres, M. R. Masouminia, R. Aminzadeh-Nik, H. Hoseinkhani, N. Olanj, Phys. Lett. B **772** (2017) 534 .
- [30] M. Modarres, M. R. Masouminia, R. Aminzadeh-Nik, H. Hoseinkhani, N. Olanj, Nucl. Phys. B **926** (2018) 406.
- [31] M. Modarres, M. R. Masouminia, R. Aminzadeh-Nik, H. Hoseinkhani, N. Olanj, Nucl. Phys. B **922** (2017) 94.
- [32] M. Modarres, R. Aminzadeh-Nik, R. Kord Valeshbadi, H. Hosseinkhani and N.Olanj, J. Phys. G **46** (2019) 105005.
- [33] N. Olanj and M. Modarres, Eur. Phys. J. C **79** (2019) 615.
- [34] H1 Collaboration, F.D. Aaron et al., Eur. Phys. J. C **65** (2010) 89.
- [35] M. A. G. Aivazis, F. I. Olness and W. K. Tung, Phys. Rev. D **50** (1994) 3085.
- [36] M. A. G. Aivazis, J. C. Collins, F. I. Olness and W. K. Tung, Phys. Rev. D **50** (1994) 3102.
- [37] J. C. Collins, Phys. Rev. D **58** (1998) 094002.
- [38] R. S. Thorne, Phys. Rev. D **73** (2006) 054019 5.
- [39] W. K. Tung, H. L. Lai, A. Belyaev, J. Pumplin, D. Stump and C. P. Yuan, JHEP **0702** (2007) 053.
- [40] *HERA* Combined Results, *HERAPDF* table,
https://www.desy.de/h1zeus/combined_results/herapdf/table.
- [41] L. Motyka and N. Timneanu, Eur. Phys. J. C, **27** (2003) 73.
- [42] L.A. Harland-Lang, A.D. Martin, P. Motylinski, R.S. Thorne, Eur. Phys. J. C **75** (2015) 204.
- [43] S. Catani, M. Ciafaloni and F. Hautmann, Phys. Lett. B, **242** (1990) 97.
- [44] S. Catani, M. Ciafaloni and F. Hautmann, Nucl. Phys. B, **366** (1991) 657.
- [45] J.C. Collins and R.K. Ellis, Nucl. Phys. B, **360** (1991) 3.
- [46] S. Catani and F. Hautmann, Nucl. Phys. B, **427** (1994) 475.
- [47] M. Ciafaloni, Phys. Lett. **356** (1995) 74.
- [48] M. A. Kimber, J. Kwiecinski, A. D. Martin and A. M. Stasto, Phys. Rev. D, **62** (2000) 094006.
- [49] K. Golec-Biernat, A. M. Stasto, Phys. Lett. B **781** (2018) 633.
- [50] G. Watt, A. D. Martin and M. G. Ryskin, Phys. Rev. D, **70** (2004) 014012.
- [51] V.S. Fadin, E.A. Kuraev, L.N. Lipatov, Phys. Lett. B **60** (1975) 50.

- [52] Ya.Ya. Balitsky, L.N. Lipatov, Sov. J. Nucl. Phys. **28** (1978) 822.
- [53] W. Furmanski, R. Petronzio, Phys. Lett. B **97** (1980) 437.
- [54] M.A. Kimber, Unintegrated parton distributions, Ph.D. Thesis, University of Durham, UK, 2001.
- [55] G.Watt, A. D. Martin, and M. G. Ryskin, Eur. Phys. J. C **31** (2003) 73.
- [56] J. Kwiecinski, A. D. Martin, and A. M. Stasto, Phys. Rev. D, **56** (1997) 3991.
- [57] ZEUS collaboration, H. Abramowicz et al., Eur.Phys.J.C, **2** (2000) 35.

a	Q^2 (GeV^2)	x	$\int_{Q_0^2}^{Q^2} \frac{dk_t^2}{k_t^2} f_a(x, k_t^2, Q^2)$	$a(x, Q^2) - a(x, Q_0^2)$	$ \Delta (\%)$
g	25	0.001	14.648	14.941	1.96
g	25	0.01	5.220	4.675	11.66
g	100	0.001	20.681	20.720	0.19
g	100	0.01	6.497	5.604	15.94
g	1000	0.001	28.089	28.630	1.89
g	1000	0.01	7.300	6.481	12.64
u	25	0.001	0.296	0.311	4.82
u	25	0.01	0.201	0.161	24.84
u	100	0.001	0.503	0.512	1.76
u	100	0.01	0.309	0.224	37.95
u	1000	0.001	0.869	0.846	2.72
u	1000	0.01	0.472	0.307	53.75
c	25	0.001	0.178	0.304	41.45
c	25	0.01	0.077	0.126	38.89
c	100	0.001	0.318	0.509	37.52
c	100	0.01	0.121	0.185	34.59
c	1000	0.001	0.586	0.847	30.81
c	1000	0.01	0.190	0.262	27.48

Table 1

TABLE I: The comparison of the k_t -integrals of the *KMR-UPDF*, by using *MMHT2014 – LO PDF* as the inputs, and their corresponding ordinary *PDF*.

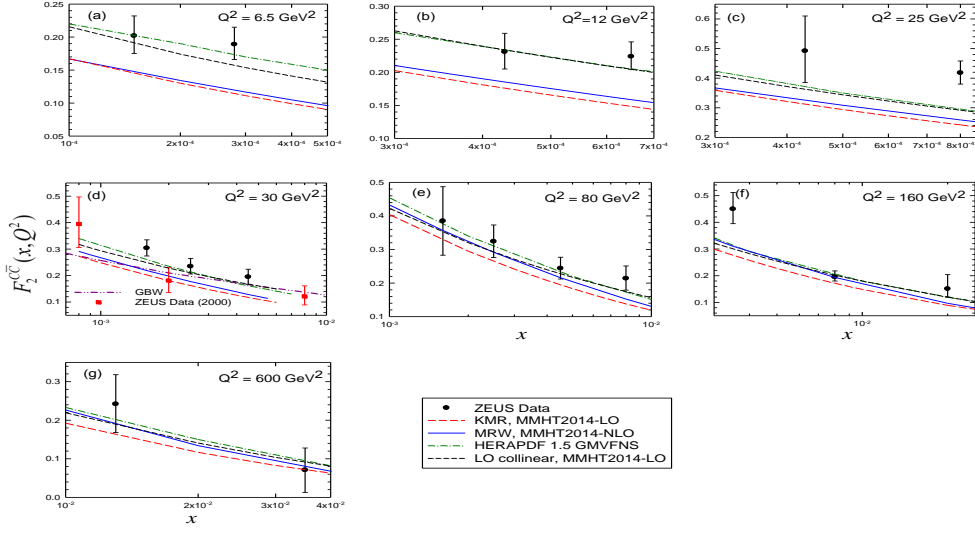


Figure 1

FIG. 1: The structure functions $F_2^{c\bar{c}}(x, Q^2)$ as a function of x for various Q^2 values for two different schemes, namely *KMR* and *MRW*. The *NLO QCD HERAPDF 1.5* [40], *GBW* [41] predictions and *ZEUS* data [5, 57] are also given. See the text for more explanations.

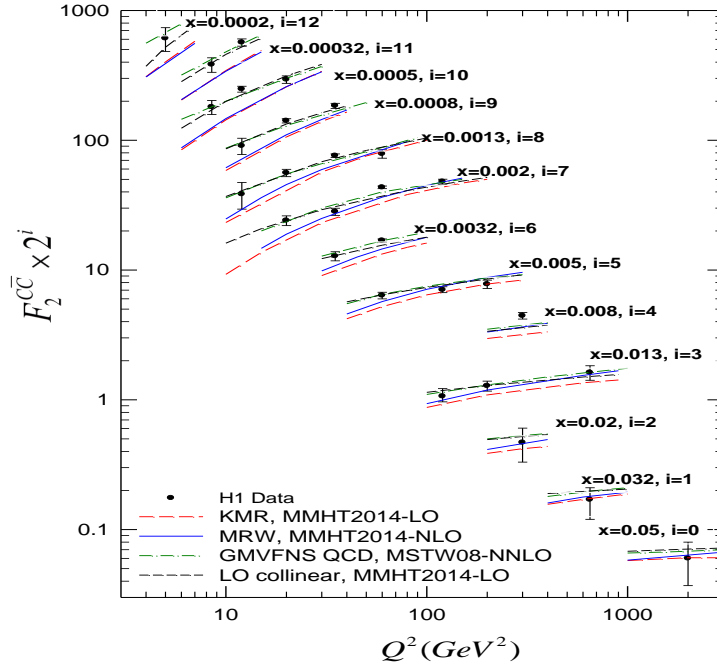


Figure 2

FIG. 2: The comparison of the charm structure functions, in the frameworks of *KMR* and *MRW* by using the *MMHT2014 – LO* and *MMHT2014 – NLO PDF* data [42], respectively, as a function of Q^2 for various x values, with the *GMVFNS QCD* predictions [35–39] of *MSTW* at *NNLO* [3] and *H1* data [34].

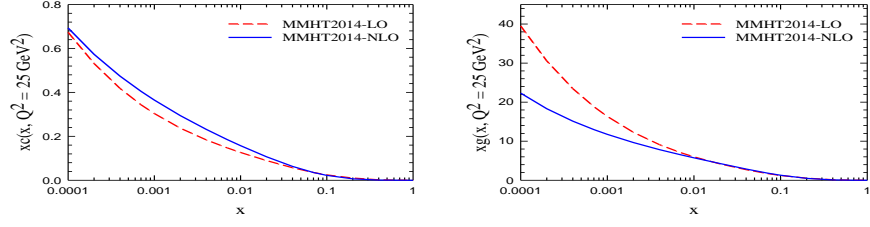


Figure 3

FIG. 3: The integrated charm quark and gluon distribution functions at scale $Q^2 = 25\text{GeV}^2$, by using the *MMHT2014-LO* and *MMHT2014-NLO* PDF data [42].

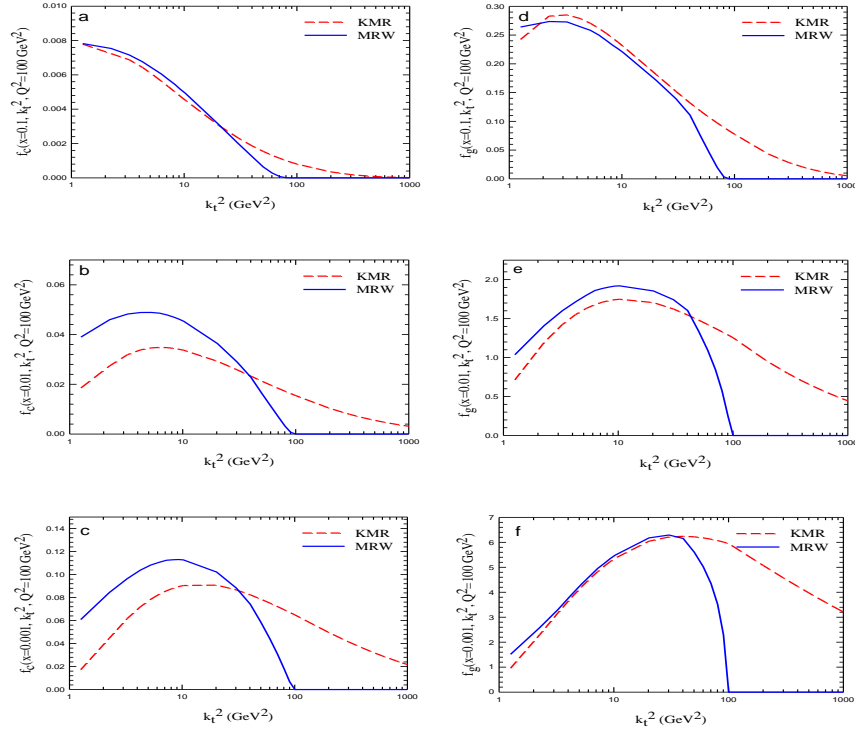


Figure 4

FIG. 4: The unintegrated charm quark and gluon distribution functions versus k_t^2 with the *KMR* (*MRW*) prescriptions by using the *MMHT2014 – LO PDF* (*MMHT2014 – NLO PDF*) as the inputs.